

## Growth of Highly Oriented Chalcocite Thin Films on Glass by Aerosol-Assisted Spray Pyrolysis Using a New Single-Source Copper Thiolate Precursor

Sven Schneider, Yu Yang, and Tobin J. Marks\*

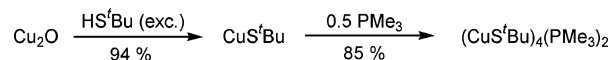
Department of Chemistry and the Materials Research Center, Northwestern University, 2145 Sheridan Road, Evanston, Illinois 60208-3113

Received June 1, 2005

Revised Manuscript Received July 6, 2005

The development of  $\text{Cu}_x\text{S}$  thin films for photovoltaics slowed in the late 1980s because of the intrinsic instability of  $\text{CdS}/\text{Cu}_2\text{S}$  heterojunction cells.<sup>1</sup> However, *n*-type semiconductors such as  $\text{TiO}_2$  and  $\text{ZnO}$  have recently been shown to yield stable *p/n* heterojunction cells with cuprous sulfide, stimulating renewed interest in high-quality  $\text{Cu}_x\text{S}$  films.<sup>2,3</sup> Among the  $\text{Cu}_x\text{S}$  phases exhibiting photovoltaic activity, monoclinic chalcocite<sup>4</sup> has the smallest band gap and conductivity.<sup>5</sup> Because the topotactic ion exchange, typically used for high-quality  $\text{CdS}/\text{Cu}_2\text{S}$  heterojunctions, is not possible for producing  $\text{Cu}_2\text{S}/\text{metal}$ –oxide heterostructures, gas-phase deposition techniques are attractive for the growth of high-quality  $\text{Cu}_2\text{S}$  thin films. Currently radio frequency (RF) sputtering of copper targets in a  $\text{H}_2\text{S}$  atmosphere<sup>6</sup> and low-pressure physical vapor deposition<sup>7</sup> are the only available gas-phase methods for growing phase-pure  $\alpha$ - $\text{Cu}_2\text{S}$  thin films.<sup>8</sup> Although the *single-source* precursor approach is very efficient for metal chalcogenide deposition by chemical vapor deposition,<sup>9</sup> no *single-source* precursors currently exist for  $\alpha$ - $\text{Cu}_2\text{S}$ .<sup>10</sup> However, in situ generated  $\text{Cu(I)}$  thiolates and mixed metal thiolate *single-source* precursors have been employed for hexagonal chalcocite nanoparticles<sup>11</sup> and  $\text{CuES}_2$

Scheme 1



(E = Ga, In) chalcocite powders and thin films,<sup>12</sup> respectively. These results raise the intriguing question of whether copper(I) thiolates could be effective precursors for growth of copper-rich chalcocite thin films. We report here on the synthesis of a new, highly soluble copper(I) thiolate *single-source* precursor and its implementation in the growth of high-quality  $\alpha$ - $\text{Cu}_2\text{S}$  thin films by aerosol-assisted spray pyrolysis.

Light-sensitive  $\text{CuS}^t\text{Bu}$  (**1**) was synthesized in high yield (Scheme 1) by a modified literature procedure (Supporting Information).<sup>13</sup> CI-MS of **1** up to  $m/z = 800$  shows tetrameric  $[\text{CuS}^t\text{Bu}]_4$  as the heaviest and major gas-phase species, a common cluster size for copper(I) thiolates in the solid state.<sup>14</sup> Atmospheric pressure thermogravimetric analysis (TGA) of **1** (Figure 1)<sup>15</sup> shows a relatively narrow thermal decomposition range (170–225 °C) with a residue of 52.0%, which is in excellent agreement with that calculated for decomposition to  $\text{Cu}_2\text{S}$  (52.1%). The calculated decomposition onset and point of maximum rate of weight loss (PMRW) are 198 and 215 °C (at 48 mass % decomposition), respectively. TGA at 0.8 Torr leaves a residue of ~8 mass % with sublimation onset (169 °C) and PMRW (187 °C, 93 mass % loss) approaching the decomposition values at atmospheric pressure. Therefore, complex **1** sublimation is accompanied by significant decomposition, and attempts to employ **1** as precursor in conventional low-pressure metal-organic CVD (LP-MOCVD) were unsuccessful, because of premature decomposition and sintering in the precursor reservoir.

Reaction of **1** with 0.5 equiv  $\text{PME}_3$  in diethyl ether affords moderately air-sensitive  $(\text{CuS}^t\text{Bu})_4(\text{PME}_3)_2$  (**2**) in >80% yield (Scheme 1; Supporting Information). Complex **2** is stable

- (1) Reynolds, D. C.; Leies, G.; Antes, L. T.; Marburger, R. E. *Phys. Rev.* **1954**, *96*, 533.
- (2) (a) Reijnen, L.; Meester, B.; Goossens, A.; Schoonman, J. *Mater. Sci. Eng.* **2002**, *C19*, 311. (b) Liu, G.; Schulmeyer, T.; Thissen, A.; Klein, A.; Jaegermann, W. *Appl. Phys. Lett.* **2003**, *82*, 2269. (c) Reijnen, L.; Meester, B.; Goossens, A.; Schoonman, J. *Chem. Vap. Deposition* **2003**, *9*, 15.
- (3) (a) Burgelman, M.; Pauwels, H. J. *Electron. Lett.* **1981**, *17*, 224. (b) Berhanu, D.; Boyle, D. S.; Govender, K.; O'Brien, P. J. *Mater. Sci.: Mater. Electron.* **2003**, *14*, 579.
- (4) Several nomenclature conventions have been used for the monoclinic chalcocite phase (JCPDS 33-0490). We employ  $\alpha$ - $\text{Cu}_2\text{S}$ , indicating the low-temperature phase of the chalcocite polymorphs: Chakrabarti, D. J.; Laughlin, D. E. In *Phase Diagrams of Binary Copper Alloys*; Subramanian, P. R., Chakrabarti, D. J., Laughlin, D. E., Eds.; ASM: Materials Park, 1994.
- (5) Nair, M. T. S.; Guerrero, L.; Nair, P. K. *Semicond. Sci. Technol.* **1998**, *13*, 1164.
- (6) (a) Armantrout, G. A.; Miller, D. E.; Vindelov, K. E.; Brown, T. G.; *J. Vac. Sci.* **1979**, *16*, 212. (b) Vanhooeck, E.; Burgelman, M. *Thin Solid Films* **1984**, *112*, 97. (c) He, Y. B.; Polity, A.; Osterreicher, I.; Pfisterer, D.; Gregor, R.; Meyer, B. K.; Hardt, M. *Physica B* **2001**, *308–310*, 1069.
- (7) Leon, M.; Terao, N.; Rueda, F. *Phys. Stat. Solidi* **1981**, *67*, K11.
- (8) Reijnen, L.; Meester, B.; de Lange, F.; Schoonman, J.; Goossens, A. *Chem. Mater.* **2005**, *17*, 2724.
- (9) (a) O'Brien, P.; Haggata, S. *Adv. Mat. Opt. Electron.* **1995**, *5*, 117. (b) O'Brien, P.; Nomura, R. *J. Mater. Chem.* **1995**, *5*, 1761. (c) Barron, A. R. *Adv. Mat. Opt. Electron.* **1995**, *5*, 245. (d) Maury, F. *Chem. Vap. Deposition* **1996**, *2*, 113. (e) Bochmann, M. *Chem. Vap. Deposition* **1996**, *2*, 85. (f) Gleizes, A. N. *Chem. Vap. Deposition* **2000**, *6*, 155. (g) Veith, M. *J. Chem. Soc., Dalton Trans.* **2002**, 2405.

- (10) (a) Nomura, R.; Miyawaki, Toyosaki, T.; Matsuda, H. *Chem. Vap. Deposition* **1996**, *2*, 174. (b) Fainer, N. I.; Romyantsev, Y. M.; Kosinova, M. L.; Yurev, G. S.; Maksimovskii, E. A.; Zemskova, S. M.; Sysoev, S. V.; Kuznetsov, F. A. *Inorg. Mater.* **1998**, *34*, 1049. (c) Kemmler, M.; Lazell, M.; O'Brien, P.; Otway, D. J.; Park, J.-H.; Walsh, J. R. *J. Mater. Sci. Mater. Electron.* **2002**, *13*, 531. (c) McCain, M. N.; Metz, A. W.; Yang, Y.; Stern, C. L.; Marks, T. J. *Chem. Vap. Deposition* **2005**, *11*, 291.
- (11) (a) Larsen, T. H.; Sigman, M.; Ghezlbash, A.; Doty, R. C.; Korgel, B. A. *J. Am. Chem. Soc.* **2003**, *125*, 5638. (b) Sigman, M. B., Jr.; Ghezlbash, A.; Hanrath, T.; Saunders, A. E.; Lee, F.; Korgel, B. A. *J. Am. Chem. Soc.* **2003**, *125*, 16050. (c) Chen, L.; Chen, Y.-B.; Wu, L.-M. *J. Am. Chem. Soc.* **2004**, *126*, 16334.
- (12) (a) Hirpo, W.; Dhinra, S.; Sutorik, A. C.; Kanatzidis, M. G. *J. Am. Chem. Soc.* **1993**, *115*, 1597. (b) Hollingsworth, J. A.; Hepp, A. F.; Buhro, W. E. *Chem. Vap. Deposition* **1999**, *5*, 105. (c) Banger, K. K.; Cowen, J.; Hepp, A. F. *Chem. Mater.* **2001**, *13*, 3827. (d) Banger, K. K.; Harris, J. D.; Cowen, J. E.; Hepp, A. F. *Thin Solid Films* **2002**, *403–404*, 390. (e) Hollingsworth, J. A.; Banger, K. K.; Jin, M. H.-C.; Harris, J. D.; Cowen, J. E.; Bohannan, E. W.; Switzer, J. A.; Buhro, W. E.; Hepp, A. F. *Thin Solid Films* **2003**, *431–432*, 63. (f) Castro, S. L.; Bailey, S. G.; Raffaelle, R. P.; Banger, K. K.; Hepp, A. F. *Chem. Mater.* **2003**, *15*, 3142.
- (13) Reifenschneider, W. U.S. Patent 3,206,466, 1965.
- (14) Janssen, M. D.; Grove, D. M.; van Koten, G. *Prog. Inorg. Chem.* **1997**, *46*, 997.
- (15) TGA analyses were carried out with 10–25 mg of the samples in alumina pans at heating rates of 3 °C/min.  $\text{N}_2$  flow rates at atmospheric pressure were adjusted to 100 mL/min.

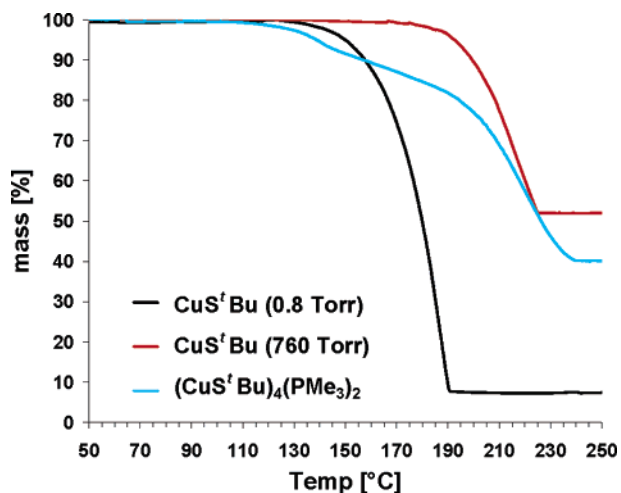


**Figure 1.** TGA traces of CuS' Bu (**1**) under N<sub>2</sub> at 0.8 Torr (black line) and at atmospheric pressure (red line) and (CuS' Bu)<sub>4</sub>(PMe<sub>3</sub>)<sub>2</sub> (**2**) at atmospheric pressure (blue line).

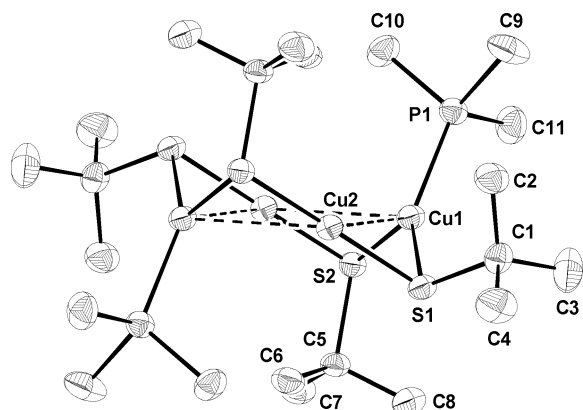


**Figure 2.** Solid-state molecular structure of (CuS' Bu)<sub>4</sub>(PMe<sub>3</sub>)<sub>2</sub> (**2**) with thermal ellipsoids drawn at the 50% probability level. Hydrogen atoms are omitted for clarity. Unlabeled atoms are related to the labeled ones via the crystallographic inversion center in the middle of the Cu<sub>4</sub> quadrangle. Selected distances (Å) and angles (deg): Cu1–Cu2, 2.8733(7); Cu1–Cu2A, 2.9483(9); Cu1–S1, 2.2331(9); Cu1–S2, 2.2970(9); Cu2–S2, 2.1603(9); Cu2–S1A, 2.1629(9); Cu1–P1, 2.2381(9); Cu2–Cu1–Cu2A, 77.55(2); Cu1–Cu2–Cu1A, 102.454(19); S1–Cu1–P1, 138.25(3); S2–Cu1–P1, 103.07(4); S1–Cu1–S2, 118.09(3); and S1A–Cu2–S2, 173.57(4).

in toluene as assessed by NMR for more than 2 weeks under N<sub>2</sub> but slowly decomposes upon exposure to light. Single-crystal X-ray diffraction (XRD) of **2** reveals a tetrameric cluster in the solid state (Figure 2; Supporting Information) similar to that of (CuS' Bu)<sub>4</sub>(PPh<sub>3</sub>)<sub>2</sub>.<sup>16</sup> Full structural details will be discussed elsewhere.<sup>17</sup> Electrospray mass-spectrometry of CH<sub>2</sub>Cl<sub>2</sub> solutions shows a cluster series [Cu<sub>x+1</sub>(S' Bu)<sub>x</sub>(PMe<sub>3</sub>)<sub>y</sub>]<sup>+</sup> having  $x \geq 4$  with the maximum size around  $x = 9$ <sup>18</sup> and no ligand chemical degradation. Therefore, aerosol-assisted spray pyrolysis should be an ideally mild delivery technique for film growth with **2**, avoiding premature precursor decomposition. TGA analysis of **2** at atmospheric pressure (Figure 1) reveals stepwise decomposition between 105 and 240 °C, leaving a residue

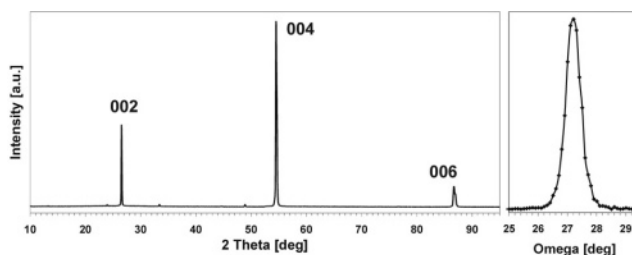


**Figure 3.** Left side:  $\theta$ – $2\theta$  XRD pattern of a 320 nm chalcocite film deposited from a toluene solution of **2** on glass at 270 °C (Cu K $\alpha$ , 1.541 Å). The 00 $l$  peak assignment refers to the hexagonal sublattice of  $\beta$ -Cu<sub>2</sub>S (JCPDS 26-1116). Right side:  $\omega$ -scan rocking curve of the film 004 peak.

(40.1 mass %) very close to that calculated for clean decomposition to Cu<sub>2</sub>S (41.7%). A first step (residue, ~90%; calculated onset, ~130 °C) is tentatively assigned to initial PMe<sub>3</sub> loss [(CuS' Bu)<sub>4</sub>PMe<sub>3</sub>], 90.0%). The shallow TGA trace leads to a rise in slope at around 200 °C/~78 mass % with the curve evolution suggesting further phosphine loss to give CuS' Bu (80.1 mass %), which is complete in the range of CuS' Bu decomposition onset. Therefore, **2** is an amply soluble CuS' Bu (**1**) source in apolar solvents and undergoes, like **1**, clean thermal decomposition to Cu<sub>2</sub>S.

The applicability of **2** as a *single-source* Cu<sub>2</sub>S precursor was demonstrated using aerosol-assisted spray pyrolysis of toluene solutions (Supporting Information). Smooth, brown, 190–320 nm thin films, strongly adherent by the “Scotch tape test”, were grown on glass substrates at 270 °C at rates of ~1.5 nm/min.  $\theta$ – $2\theta$  XRD scans of the films (Figure 3) can be indexed in the hexagonal  $\beta$ -Cu<sub>2</sub>S lattice (*high*-chalcocite, JCPDS 26-1116) with a high preferential 00 $l$  orientation as observed for reactively RF-sputtered Cu<sub>2</sub>S films.<sup>6</sup> The  $\omega$ -scan rocking curve of the 004 peak (fwhm = 0.6°) further documents the extremely high out-of-plane orientation of the films on an amorphous substrate. However,  $\beta$ -Cu<sub>2</sub>S films undergo reversible phase transitions around 80 °C to monoclinic *low*-chalcocite Cu<sub>x</sub>S (1.997 ≤  $x$  ≤ 2.000) or *pseudo*-orthorhombic djurleite (1.942 ≤  $x$  ≤ 1.988) phases,<sup>19</sup> both representing superstructures with only marginal distortions of the hexagonal  $\beta$ -Cu<sub>2</sub>S anion sublattice.<sup>20</sup> Therefore, 00 $l$  ordered  $\beta$ -Cu<sub>2</sub>S films are not easily distinguished from  $\alpha$ -Cu<sub>2</sub>S or djurleite by  $\theta$ – $2\theta$  scans. In the present work, XRD of the powder detached from the substrate by ultrasonication identifies the material as monoclinic  $\alpha$ -Cu<sub>2</sub>S (JCPDS 33-0490).<sup>21</sup>

A scanning electron microscopic (SEM) image of a typical film reveals large plates with in-plane dimensions in the ~1–2  $\mu$ m range (Figure 4). Note that the grain boundaries are oriented parallel to the substrate normal, separating hexagonally-shaped microplatelets. Both the crystallographic orientation and the film microstructure, therefore, suggest an island growth mechanism. The root-mean-square (rms) roughness by atomic force microscopy of single grains is as low as 1–3 nm over an area of 1–2  $\mu$ m<sup>2</sup>, in accord with

(16) Dance, I. G.; Guernsey, P. J.; Rae, A. D.; Scudder, M. L. *Inorg. Chem.* **1983**, *22*, 2883.

(17) Schneider, S.; Marks, T. J. Manuscript in preparation.

(18) As a result of the identical mass of the fragments [CuS' Bu] and [PMe<sub>3</sub>]<sub>2</sub> ( $m/z = 152$ ), cluster peaks larger than [Cu<sub>(x+1)-n</sub>(S' Bu)<sub>x-n</sub>(PMe<sub>3</sub>)<sub>n</sub>] could not be unambiguously assigned.

(19) (a) Leon, M.; Terao, N.; Rueda, F. *Phys. Stat. Solidi.* **1981**, *67*, K11. (b) Leon, M. *J. Mater. Sci.* **1990**, *25*, 669.

(20) Evans, H. T., Jr. *Z. Kristallogr.* **1979**, *150*, 299.

(21) A weak peak in the films at  $2\theta = 33.4^\circ$  is occasionally observed, especially for films with  $d < 150$  nm, and is assigned to the [1000] peak of a djurleite trace impurity. The 00 $l$  orientation of  $\beta$ -Cu<sub>2</sub>S transforms to the  $h00$  orientation in the djurleite superstructure.

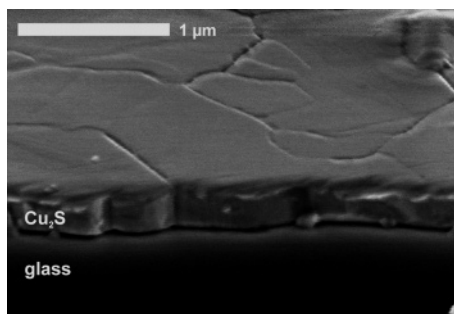


**Figure 4.** Cross-sectional SEM image of a 320 nm chalcocite film on glass.

highly uniform growth. The rms film roughness over  $25 \mu\text{m}^2$  is  $\sim 10$  nm.

No features of C, O, or P impurities are detected in the  $\text{Cu}_2\text{S}$  films by X-ray photoelectron spectroscopy after cleaning the surface by brief  $\text{Ar}^+$  sputtering (15 min/ $\sim 45$  Å). All Cu peaks are free of satellites, implying the absence of  $\text{Cu}^{\text{II}}$ .<sup>22</sup> The binding energies of the Cu  $2p_{3/2}$  and  $2p_{1/2}$  (932.8 eV, 953.1 eV) and S 2p features (161.8 eV) are in agreement with those of bulk  $\text{Cu}_2\text{S}$ .<sup>23</sup> Electrical properties were characterized by four-probe and Hall-effect measurements at room temperature. Conductivities, Hall mobilities, and hole concentrations are in the range of 16–32 S/cm, 3.2–4.2  $\text{cm}^2/(\text{V s})$ , and  $2.3\text{--}6.2 \times 10^{19} \text{ cm}^{-3}$ , respectively. Heavy p-type doping was similarly observed in RF-sputtered  $\alpha\text{-Cu}_2\text{S}$  films.<sup>6c,24</sup> The hole concentration in chalcocite is linearly related to copper vacancies at the valence band edge which

act as acceptors with high ionization probabilities.<sup>24b</sup> This suggests our films to be in the compositional range  $\text{Cu}_{1.999}\text{S}\text{--}\text{Cu}_{1.997}\text{S}$ . Indirect (1.4 eV) and direct (2.2 eV) band gaps of a 320 nm film were estimated by transmission optical spectroscopy from  $(\alpha h\nu)^{1/2}$  vs  $h\nu$  and  $(\alpha h\nu)^2$  vs  $h\nu$  plots and agree well with the band gaps of  $\alpha\text{-Cu}_2\text{S}$  single crystals along the same crystallographic axis.<sup>25</sup>

In conclusion, we presented the synthesis, characterization, and thermal stability characteristics of phosphine complex **2** as a soluble source of polymeric **1**. The efficacy as the first *single-source* precursor for deposition of  $\alpha\text{-Cu}_2\text{S}$  was demonstrated by aerosol-assisted spray pyrolysis growth of phase-pure,<sup>21</sup> highly textured chalcocite thin films on glass. The good organic solvent solubility suggests further utility of **2**, for example, for the preparation of cuprous sulfide nanoparticles or  $\text{Cu}_2\text{S}$ /polymer hybrid structures. These results support a general applicability of phosphine-stabilized copper(I) thiolates as a new class of *single-source*  $\text{Cu}_2\text{S}$  precursors.

**Acknowledgment.** We thank the NSF MRSEC program for support of this research (DMR-0076097) and C.L. Stern for single-crystal X-ray data acquisition. S.S. thanks the DFG for a postdoctoral fellowship under the Emmy Noether-Programm.

**Supporting Information Available:** Synthetic schemes and analytical data for **1** and **2**, X-ray structural information on **2**, and film growth and characterization details (PDF). X-ray crystallographic file of **2** (CIF). This material is available free of charge via the Internet at <http://pubs.acs.org>.

CM051175G

(22) Frost, D. C.; Ishitani, A.; McDowell, C. A. *Mol. Phys.* **1972**, *24*, 861.

(23) Bhide, V. G.; Salkalachen, S.; Rastogi, A. C.; Rao, C. N. R.; Hedge, M. S. *J. Phys. D: Appl. Phys.* **1981**, *14*, 1647.

(24) (a) Leong, J. Y.; Yee, J. H. *Appl. Phys. Lett.* **1979**, *35*, 601. (b) Wagner, R.; Wiemhöfer, H.-D. *J. Phys. Chem. Solids* **1983**, *44*, 801

(25) Mulder B. *J. Phys. Stat. Solidi* **1973**, *15*, 409.